ELSEVIER

Journal of Chromatography A, 828 (1998) 59–73

JOURNAL OF CHROMATOGRAPHY A

Characterization of silica-based octyl phases of different bonding density
Part II. Studies of surface properties and chromatographic selectivity

Y. Bereznitski, M. Jaroniec*, M.E. Gangoda

Separation and Surface Science Center, Chemistry Department, Kent State University, Kent, OH 44242, USA

Abstract

The goal of the current work was to evaluate changes in the surface composition of the stationary phase as a function of the bonded ligand density. To fulfill this purpose several octyl phases of different surface coverage were synthesized from the same support silica. For each chromatographic system the methylene selectivity measurements were used to estimate the equilibrium sorption constant and surface excess of acetonitrile in the stationary phase. The differences in the stationary phase composition were correlated with the surface properties of the corresponding chromatographic packings, which were characterized by nitrogen adsorption, thermogravimetry and solid-state NMR.

Keywords: Silica; Stationary phases, LC; Octyl stationary phases; Selectivity; Surface composition

1. Introduction

High-performance liquid chromatography under reversed-phase conditions is an extremely powerful an versatile analytical technique [1–3]. The importance of this method can hardly be overestimated. However, inspite of a large number of practical applications and a variety of commercially available reversed-phase columns, the retention mechanism and underlying principles of reversed-phase chromatography are subject of current discussion in scientific literature [4,5].

At present most of the chromatographic theories agree that both mobile phase and stationary phase play an active role in establishing the retention mechanism under reversed-phase conditions [4–6]. The stationary phase is seen as a dynamic, heterogeneous medium the properties of which are strongly affected by such factors as chemical nature of silica support and its pretreatment, type of the attached ligands and their density, secondary bonding effects and end-capping. In turn, chromatographic behavior of the stationary phase determined by such factors as configuration of the ligand chains, intercalation of solvent into the bonded layer, and activity of residual silanols depends also on the properties of the mobile phase. Therefore, in order to understand the retention process and optimize chromatographic separations it is important to study the properties of chromatographic packings, especially the surface composition

*Corresponding author. Tel.: +1-330-672-3790; Fax: +1-330-672-3816; E-mail: jaroniec@scorpio.kent.edu

0021-9673/98/$ – see front matter
PII: S0021-9673(98)00830-9

of the stationary phase as a function of the mobile phase composition.

Previous studies have indicated that such factors as structural and chemical heterogeneity of silica surface, amount and type of surface silanols, chemical nature and density of the chemically bonded ligand can affect composition of the stationary phase [7–15]. The objective of this work was to study the surface excess as a function of the bonded ligand density. For this purpose several octyl phases of various surface coverage were synthesized from the same silica support. For each chromatographic system the methylene selectivity measurements were used to estimate the equilibrium sorption constant and the surface excess of acetonitrile in the stationary phase. The differences in the stationary phase composition were correlated with surface and structural properties of the chromatographic packings studied, which were characterized by nitrogen adsorption, thermogravimetry and solid state NMR.

2. Experimental

2.1. Materials

Chromatographic silica gel Luna (batch 35 119) was donated by Phenomenex (Torrance, CA, USA). According to manufacturer's information, it has an average pore diameter of 10 nm, and particle size of 5 μm.

The silanizing agent, *n*-octyldimethylchlorosilane, was obtained from Huls (Piscataway, NJ, USA). Test solutes (namely, benzene, methylbenzene, ethylbenzene, propylbenzene, butylbenzene), acetone, pyridine, methanol were bought from Aldrich (Milwaukee, WI, USA). The reaction solvent, toluene of ACS grade, was purchased from Fisher (Pittsburgh, PA). All reagents were used as received.

For column packing and chromatographic experiments the high-performance liquid chromatography solvents such as methanol, acetonitrile, 2-propanol were purchased from Fisher. The mobile phases of various composition were prepared by manually mixing acetonitrile with deionized water. Water was in-house purified using the Milli-Q system produced by Millipore (Milford, MA). All mobile phases were outgassed before use.

2.2. Synthesis of C_8 bonded phases

Chemically-bonded phases of different bonding density were synthesized via reaction of silica with *n*-octyldimethylchlorosilane [16]. The reaction was done in toluene under refluxing conditions. A post-reaction curing step was used for all synthesized octyl phases in order to improve their stability and increase surface coverage. The specific details of the synthetic procedure are described in Part I of this paper.

2.3. Elemental analysis

Control of the pyridine impurities and determination of carbon percentage in the modified silica samples was done using a CHNS-932 elemental analyzer produced by LECO (St. Joseph, MI, USA). The surface coverage of octyl phases was calculated from the carbon content data using the well-known equation described elsewhere [17].

2.4. Column packing

Approximately 2.7 g of the chemically modified silica and 30 ml of 2-propanol were stirred together to form a slurry. The 100 mm×4.0 mm I.D. stainless steel columns were packed in upward flow of the delivery solvent using a dynamic slurry method. The columns were packed under the pressure of 6000 p.s.i. employing a Haskel (Burbank, CA, USA) DSTV-52C air-driven fluid pump (p.s.i.=6894.76 Pa). Methanol was used as a delivery solvent.

2.5. Chromatographic measurements

Chromatographic retention measurements were carried out on Varian (Walnut Creek, CA, USA) modular liquid chromatograph which consisted of Varian 9012 solvent delivery system, Varian 9100 autosampler, Varian 9050 variable-wavelength UV–Vis detector, Varian Mistrel column oven, and Rheodyne 8025 (Berkeley, CA) injection valve equipped with a 20 μl loop.

All experiments were carried out at 25°C and a flow-rate of 1 ml/min. The detector was set to a wavelength of 254 nm. Data acquisition was done using Varian Star Chromatography Workstation. The

retention data for a series of alkyl benzenes, from benzene to butyl benzene, were measured using different compositions of the acetonitrile–water eluent. Determination of the void volume was done using solvent disturbance peak.

2.6. Evaluation of the surface excess

According to the partition-displacement model, the natural logarithm of the methylene selectivity, s, can be expressed by the following equation [7–9]:

$$s = \phi_o^{\sigma} s_o + \phi_w^{\sigma} s_w \quad (1)$$

where ϕ_o^{σ} and ϕ_w^{σ} are, respectively, the volume fractions of organic solvent and water in the stationary (surface) phase, and $\phi_o^{\sigma} + \phi_w^{\sigma} = 1$, because the solute's concentration is infinitely low. The symbols s_o and s_w denote the logarithmic methylene selectivities in the pure organic solvent and water, respectively. Their values can be determined from the $s(\phi_o^{1})$ plot by extrapolating ϕ_o^{1} to unity and zero, respectively. The values of the methylene selectivity, s, can be used to calculate the excess selectivity, s_e:

$$s_e = s - s_o \phi_o^{1} - s_w \phi_w^{1} = A(\phi_o^{\sigma} - \phi_o^{1}) \quad (2)$$

where $(\phi_o^{\sigma} - \phi_o^{1})$ is the surface excess of the organic component in the stationary phase, ϕ_o^{1} is the volume fraction of the organic component in the mobile phase, and A is the proportionality constant.

The volume fraction of the organic component in the stationary phase, ϕ_o^{σ}, is a function of the mobile phase composition, ϕ_o^{1} . For the ideal phases the volume fraction ϕ_o^{σ} can be evaluated analytically using the Everett's equation for competitive adsorption from solutions [18]:

$$\phi_o^{\sigma} = \frac{K_{ow}\phi_o^{1}}{(1 - \phi_o^{1} + K_{ow}\phi_o^{1})} \quad (3)$$

where K_{ow} is the equilibrium constant which describes the competitive sorption of solvents on the stationary phase.

By substituting ϕ_o^{σ} in Eq. (1) by Eq. (3) the following expression can be obtained:

$$s = s_w - (s_w - s_o)\frac{K_{ow}\phi_o^{1}}{(1 - \phi_o^{1} + K_{ow}\phi_o^{1})} \quad (4)$$

In this expression the only parameter unknown is K_{ow}. It can be evaluated by fitting the experimental $s(\phi_o^{1})$ data by Eq. (4), or its linear form:

$$\frac{1}{s_w - s} = \frac{K_{ow} - 1}{K_{ow}(s_w - s_o)} + \frac{1}{K_{ow}(s_w - s_o)}\frac{1}{\phi_o^{1}} \quad (5)$$

Once the value of the equilibrium adsorption constant is known, Eq. (3) can be used to calculate the surface excess of the organic component in the stationary phase, i.e. $(\phi_o^{\sigma} - \phi_o^{1})$.

2.7. Adsorption measurements

Measurements of nitrogen adsorption isotherms were carried out at −195.5°C using a model ASAP 2010 volumetric sorption analyzer from Micromeritics, Inc., (Norcross, GA, USA). Prior to making sorption measurements carbon samples were outgassed at 200°C for 2 h under the vacuum pressure of 10^{-4} Torr (1 Torr = 133.322 Pa).

The standard analysis of adsorption isotherms included evaluation of the specific surface area according to the BET method [19] and the total pore volume using the single point method [19]. The t-plot method was used to investigate the presence of micropores [19]. The pore size distributions were calculated according to the BJH method [20].

Additionally, an advanced numerical algorithm employing a regularization procedure was applied to evaluate the adsorption energy distributions (AEDs) for the silica samples studied. The adsorption energy distributions were calculated from the submonolayer range of the adsorption isotherms using the INTEG software [21]. The local adsorption was modeled by the Fowler–Guggenheim equation for random distribution of adsorption sites. In this model the number of nearest neighbors was assumed to be four ($z = 4$), and the value of the interaction energy parameter $\omega/k = 95$ K was used to calculate the adsorption energy distribution by inverting the integral equation of adsorption described elsewhere [22].

2.8. Solid-state NMR experiments

The variable contact time ^{1}H–^{29}Si-cross polarization (CP) magic angle spinning (MAS)-NMR experiments were performed on Bruker DMX 400WB

spectrometer (USA Bruker Instruments, San Jose, CA, USA) with ^{29}Si Larmor precession frequency of 79.5 MHz. The samples were packed in 9 mm zirconia rotor and spun at MAS frequency of 2000 Hz using dry air as driving and bearing gas. The experiment temperature was controlled at 25°C. The proton 90° pulse length was set to 4 μsec. The TMS was used as an external chemical shift reference. CP performance was optimized using 3-(trimethylsilyl)-1-propane sulfonic acid sodium salt (DSS). Line broadening of 50 Hz was applied in all spectra.

For each sample 32 spectra corresponding to different contact times (from 0.2 to 100 μs) were collected. For most spectra 400 FIDs were accumulated in 2 K data points using the acquisition time of 43 ms and cycle delay time of 5 s.

For each silica the analysis of signal intensities as a function of contact time was performed using the following equation [23]:

$$I(t) = I_0 \exp(-t/T_{1\rho\mathrm{H}})[1 - \exp(-(1 - T_{\mathrm{SiH}}/T_{1\rho\mathrm{H}})t/T_{\mathrm{SiH}}]/(1 - T_{\mathrm{SiH}}/T_{1\rho H}) \quad (6)$$

Fitting experimental CP curves with Eq. (6) yields the values of the cross-polarization time constant T_{SiH}, the relaxation time of the proton in rotating frame $T_{1\rho H}$, and the maximum obtainable magnetization I_0. The ratio of magnetization parameters [24] $I_0(Q_2)$:$I_0(Q_3)$:$I_0(Q_4)$ was used to calculate the percent fractions of the silicon groups. It should be mentioned that due to the surface selectivity of the CP sequence the bulk Q_4 groups are not detected. However, the inner chromatographically inaccessible silanol groups (typically found in fine micropores) also contribute to the overall intensity of the Q_2 and Q_3 signals, but the studies of deuterium exchanged silica samples indicate that their number is small [25].

3. Results and discussion

3.1. CP-MAS-NMR studies

The variable contact time CP-MAS-NMR experiments were conducted on the original and derivatized silica samples. A typical CP curve obtained for non-modified Luna sample is shown in Fig. 1. For each sample the analysis of cross-polarization curves was done using Eq. (5) to determine values for the cross-polarization time constant T_{SiH}, the relaxation time of the proton in rotating frame $T_{1\rho H}$, and the maximum obtainable magnetization I_0. These data are summarized in Table 1.

Analysis of the relaxation parameters obtained from Eq. (6) allows to obtain structural information about the silica gels studied. Thus, the cross-polarization times (T_{SiH}) for Q_2 and Q_3 signals are short and comparable in magnitude (about 2 ms for most of the samples). Considering a strong distance dependence of the dipolar interactions the short T_{SiH} times indicate that silicon atoms and protons are located in close geometrical proximity. On the other hand, the cross-polarization time constant for Q_4 signals is substantially larger than T_{SiH} for Q_2 and Q_3 signals, which proves that cross-polarization source (the proton) is located much further away from the silicon atom in siloxane group. The information about mobility of cross-polarizing protons is manifested in parameter $T_{1\rho H}$. The magnitude of $T_{1\rho H}$ parameter is dependent on fluctuations in the magnetic field of protons due to their motion. The shorter $T_{1\rho H}$ relaxation times indicate the greater mobility of protons. For all samples studied $T_{1\rho H}(Q_2) < T_{1\rho H}(Q_4)$, which demonstrates greater mobility of protons involved in cross-polarization of silicon atoms in geminal groups.

The ratio of maximum magnetizations for Q_2, Q_3, and Q_4 signals was used to calculate the percent fractions of the respective groups in each silica sample (Table 2). These data were plotted as a function of the surface coverage of octyl phase. As can be seen in Fig. 2 the fraction of siloxane groups steadily increases as a function of the surface coverage, which indicates more surface hydroxyls being converted to siloxanes as a result of surface derivatization. On the other hand, the fraction of geminal groups decreases from initial 7.1(2)% in non-modified Luna sample to 5.1(2)% in Luna-1.20 sample and remains practically unchanged for Luna-1.60 sample. As the surface coverage increases to 3.32 $\mu\mathrm{mol}/\mathrm{m}^2$ the fraction of geminal silanols drops to 3.5(6)%. In contrast to that, the fraction of isolated silanols slightly increases from 42.6(3)% in non-modified sample to 43.3(5)% in Luna-1.20. As

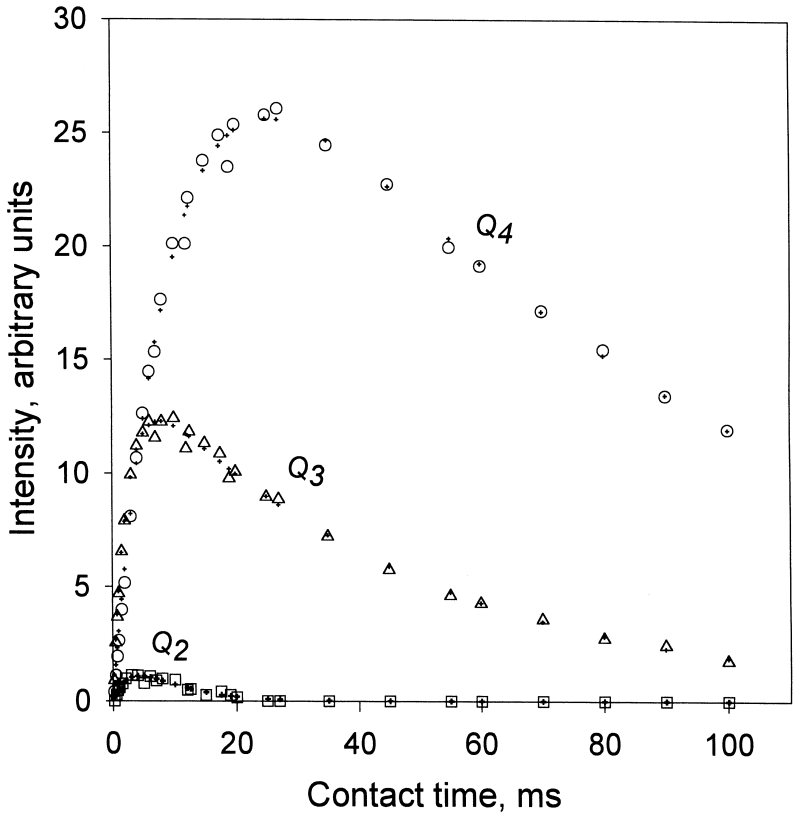

Fig. 1. ^{1}H-^{29}Si-CP-MAS-NMR cross-polarization curves for Luna-3.32 sample.

the surface coverage almost triples the Q_3 fraction decreases to 27.6(8)% in Luna-3.32. Such tendencies may indicate somewhat higher activity of the geminal silanols in reaction with octyldimethylchlorosilane. As the surface coverage increases the amount of geminal groups decreases,

Table 1
Analysis of the CP-MAS-NMR cross-polarization curves for the samples studied according to Eq. (5)

Coverage μmol/m^2	Signal type	Equation parameters		
		I_0 (arb. units)	$T_{1\rho H}$ (ms)	T_{SiH} (ms)
0.00	Q_2	4.1(1)	25.6(1.6)	2.0(2)
	Q_3	24.5(2)	58.8(1.3)	2.23(6)
	Q_4	28.9(4)	78.0(2.1)	11.4(3)
1.20	Q_2	1.32(5)	13.9(9)	0.71(8)
	Q_3	11.3(1)	28.2(6)	1.02(3)
	Q_4	13.5(2)	63.5(2.3)	5.5(2)
1.60	Q_2	2.3(1)	34.0(3.5)	2.8(3)
	Q_3	13.7(3)	93.2(6.4)	3.3(2)
	Q_4	26.5(1.2)	71.6(5.4)	18.9(1.1)
3.32	Q_2	1.8(3)	7.4(1.6)	2.4(4)
	Q_3	14.5(2)	47.2(1.2)	2.50(7)
	Q_4	34.9(8)	82.2(3.6)	10.9(4)

Table 2
Relative abundances of different silicon groups

Coverage (μmol/m^2)	$I_0(Q_2)$:$I_0(Q_3)$:$I_0(Q_4)$	Q_2 (%)	Q_3 (%)	Q_4 (%)
0.00	4.1(1):24.5(2):28.9(4)	7.1(2)	42.6(5)	50.3(8)
1.20	1.32(5):11.3(1):13.5(2)	5.1(2)	43.3(5)	51.7(9)
1.60	2.3(1):13.7(3):26.5(1.2)	5.4(3)	32.2(1.1)	62.3(3.3)
3.32	1.8(3):14.5(2):34.9(8)	3.5(6)	28.3(6)	68.2(1.9)

and they become less accessible for modification. Consequently, the silanol molecules react mostly with more abundant isolated silanols (Q_3-sites). Thus, the analysis of cross-polarization curves allows to obtain quantitative information about changes in the populations of different silicon groups introduced upon derivatization of the silica surface. However, it should be noted that quantitative changes obtained via such analysis may not adequately describe the stoichiometry of the reaction process due to curve-fitting errors and a simplified description of cross-polarization process given by Eq. (6) [23].

3.2. Adsorption studies

Nitrogen adsorption measurements were performed to gain information on the structural and surface properties of the original and modified Luna samples. Thus, the carbon content data obtained from elemental analysis together with the specific surface area of the original (non-modified) Luna sample determined from nitrogen adsorption were used to calculate the surface coverage of octyl phase for the modified samples [17]. These data are presented in Table 3.

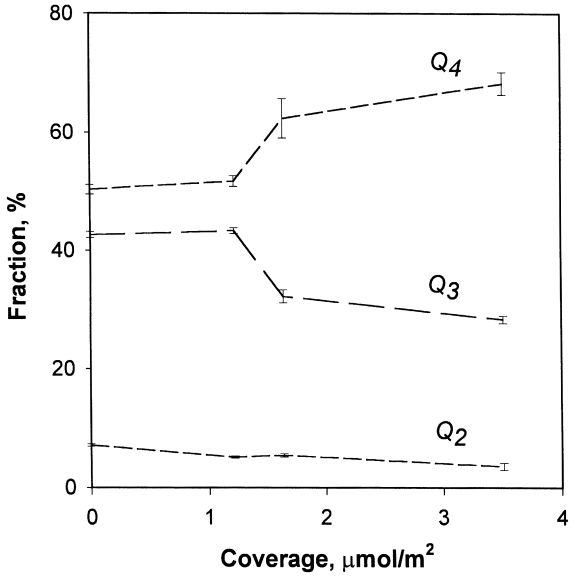

Fig. 2. Fractions of different silicon groups as a function of surface coverage.

Complete nitrogen adsorption–desorption isotherms for original and modified samples are shown in Fig. 3. According to IUPAC classification [26], these adsorption isotherms can be classified as type IV, which reflects formation of the adsorption monolayer followed by multilayer adsorption and capillary condensation. An increase of the surface coverage resulted in a gradual decrease in the adsorption capacity for the modified samples. Nonetheless, all adsorption isotherms exhibited a well-defined H1 type hysteresis loop [26]. This fact is important for chromatographic applications, because it indicates mesoporous structure of the modified samples. Moreover, the H1 type is characteristic for porous materials consistent of uniform spherical particles with narrow distribution of particle and pore sizes.

The results of the qualitative analysis of adsorption isotherms are supported by calculations of the BJH pore size distributions, which are shown in Fig. 4. An increase in the surface coverage of the octyl phase resulted in a shift of the PSD maximum

Table 3
Elemental analysis and adsorption characterization of the silica gels studied

Coverage (μmol/m^2)	S_{BET} (m^2/g)	Carbon (%)	V_t (cm^3/g)	$\varnothing_{BJH}$ (nm)
0.00	465	0	1.17	9.20
1.20	400	6.12	1.00	7.94
1.60	384	7.91	0.90	7.50
3.32	297	14.66	0.70	7.00

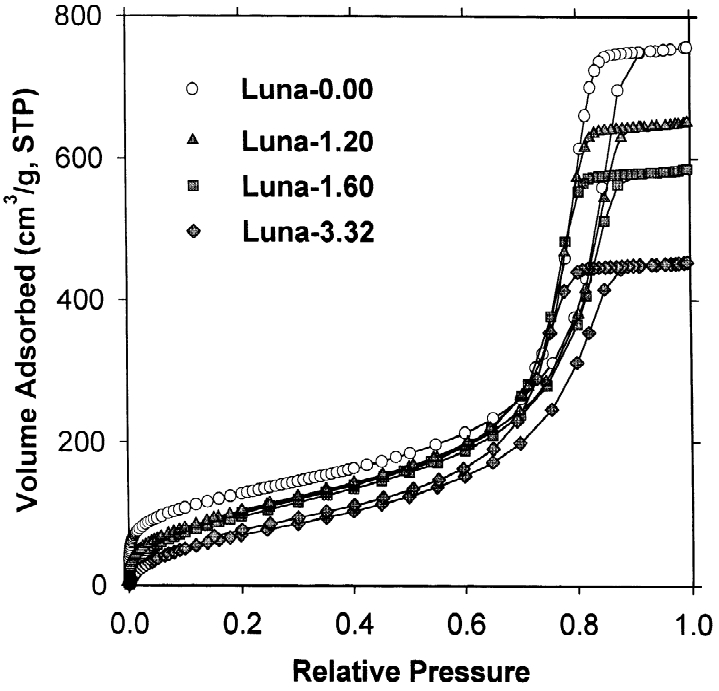

Fig. 3. Nitrogen adsorption–desorption isotherms for the original and derivatized silica samples measured at −195.5°C.

towards smaller pore diameters as well as in an overall decrease in the total pore volume. A systematic decrease in the pore diameters proves that surface modification indeed took place inside of the mesopores. Quantitatively, the average BJH pore diameter decreased from 9.20 nm to 7.00 nm for Luna-0.00 and Luna-3.32, respectively. Similar correlation with the surface coverage was observed for other standard quantities such as the BET specific surface area and the total pore volume. Thus, the specific surface area decreased from 465 to 297 m^2/g, and the total pore volume reduced from 1.17 to 0.70 cm^3/g for Luna-0.00 and Luna-3.32 samples, correspondingly.

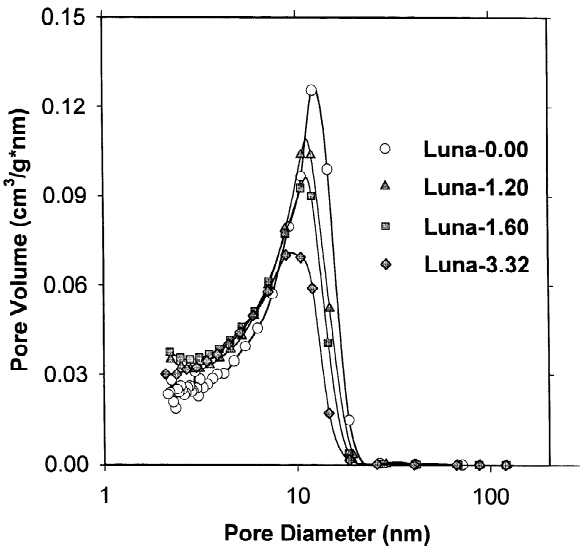

Fig. 4. BJH pore size distributions for the silica gels studied.

In addition to the above characterization methods the t-plot method was applied for analysis of adsorption isotherms to probe the samples for a presence of micropores, which can negatively affect mass-transfer properties of the chromatographic packings studied. An application of the t-plot method provided no substantial evidence for the presence of micropores. This result is supported by an observation of the overall shape of adsorption isotherms in the low pressure region. Thus, in this range (10^{-5}–10^{-6} P/P_0) adsorption isotherms of microporous samples typically exhibit a sharp kink due to a high

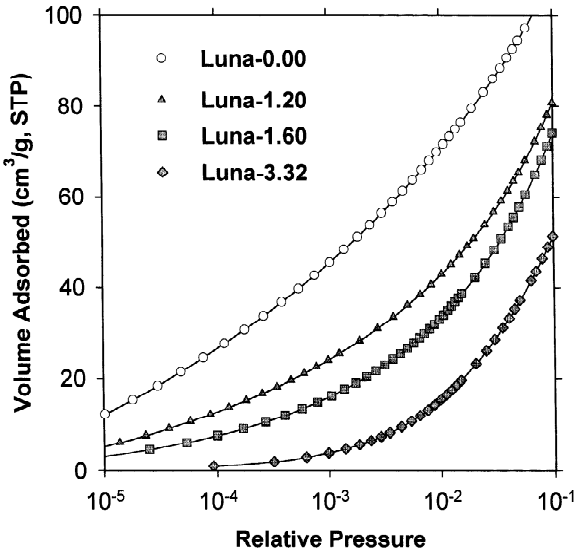

Fig. 5. Low pressure nitrogen adsorption isotherms on the silica gels studied shown in the logarithmic scale.

adsorption potential in micropores. However, as can be seen in Fig. 5, all adsorption isotherms in the low pressure region gradually change as a function of the relative pressure.

The low pressure region of adsorption isotherms provides direct information about surface properties of the silica gels studied. A sub-monolayer range of adsorption isotherms was used to calculate the AEDs for original and modified samples. This calculation was done by inverting the integral equation of adsorption [22], in which Fowler–Guggenheim (FG) equation was used to represent the local adsorption on the surface with a random distribution of adsorption sites. In the FG equation the number of nearest neighbors was assumed to be four, and the interaction energy parameter was set to 95 K [21]. Numerically stable solutions of the integral equation of adsorption were obtained for the regularization parameter equal to 10^{-2}.

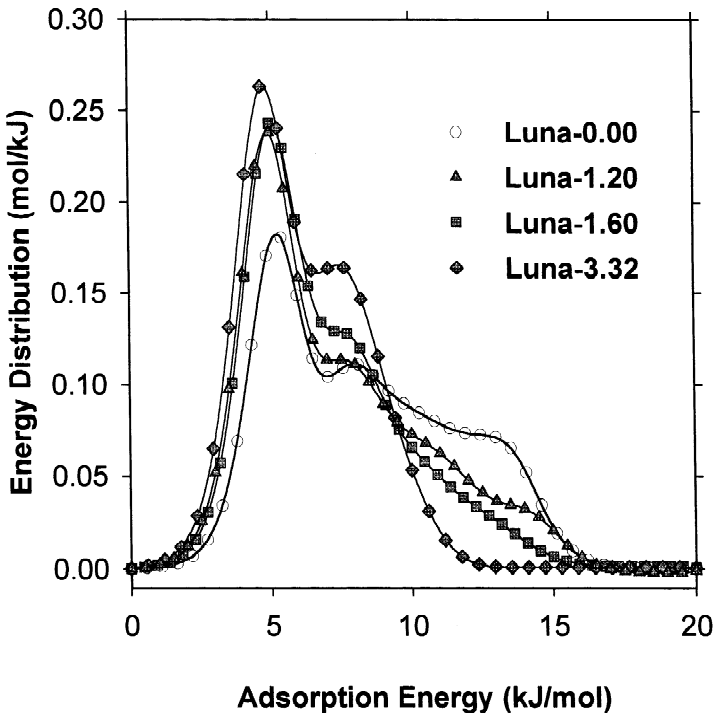

Fig. 6. Adsorption energy distributions (AEDs) for the silica gels studied.

Adsorption energy distribution functions for original and modified Luna samples are shown in Fig. 6. The AED for Luna-0.00 is the widest. It consists of at least three overlapping peaks, which cover energy range from 2 to 17 kJ/mol. Such wide spectrum of adsorption energies is typical for heterogeneous surface of bare silica [27,28]. As the surface coverage of the octyl phase becomes more dense, the AED spectra undergo definite changes. The intensity of the high energy peak centered at 14 kJ/mol gradually decreases in the AED spectra of Luna-1.20 and Luna-1.60 samples. Finally, this peak practically disappears in the distribution function of Luna-3.32 sample. The disappearance of the high energy peak is clearly related to the effect of surface modification, which results in the diminishing amount of high adsorption energy sites available for interactions with adsorbate molecules. The silica surface becomes less heterogeneous, which makes it more advantageous for chromatographic applications. As shown in the NMR section, the silanization decreases the amount of surface hydroxyls, which are transformed in Si–O–Si_s bonds during the reaction with octyldimethylchlorosilane. Thus, despite the apparent difference in the physical nature of interactions at the gas–solid interface (adsorption studies) from those at the liquid–solid interface (chromatography studies), the analysis of the adsorption energy distributions proves to be a valuable tool for evaluating the changes in the surface properties of chromatographic packings introduced through modification of the silica surface.

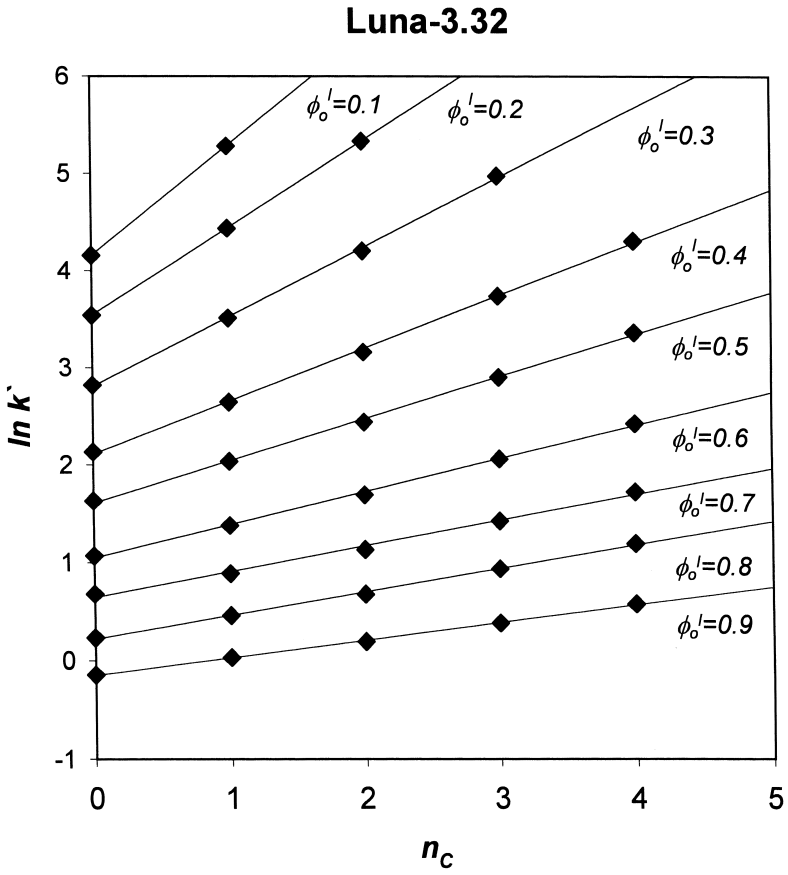

Fig. 7. Natural logarithm of the capacity factor for Luna-3.32 octyl phase as a function of the number of carbon atoms in the alkyl chain of homologous solutes.

3.3. Chromatographic studies

Retention of homologous alkylbenzenes was studied on C_8 columns packed with chromatographic silicas of different degree of surface coverage. In chromatographic experiments composition of the mobile phase varied from 10 to 90% (v/v) of acetonitrile. For each chromatographic system the logarithm of the capacity factor k' showed a linear dependence on the number of carbon atoms in the alkyl chain of test solutes, n_c. A typical plot of the ln k' dependence on n_c obtained for Luna-3.32 octyl phase is shown in Fig. 7. As can be noticed, the retention and correspondingly the ln k' for each alkylbenzene progressively increased as the concentration of acetonitrile in the mobile phase was reduced. Such dependence is typical for many reversed-phase systems described in literature [3], and for many of them it has almost linear character. This phenomenon is explained by a decrease in the elution strength of the mobile phase due a reduced concentration of acetonitrile.

A similar tendency was observed for the other octyl phases (see Figs. 8 and 9). However, at high concentrations of water in the mobile phase the retention behavior of analytes, especially those with shorter alkyl chains, started to deviate from a general pattern. Thus, for Luna-1.60 the retention of benzene in the mobile phase containing 10% of acetonitrile was almost the same as in 20% solution. For Luna-1.20 phase the retention of benzene in 10% acetonitrile was less than that in 20% acetonitrile. In order to confirm this tendency an additional measurement was done for Luna-1.20 in the mobile phase con-

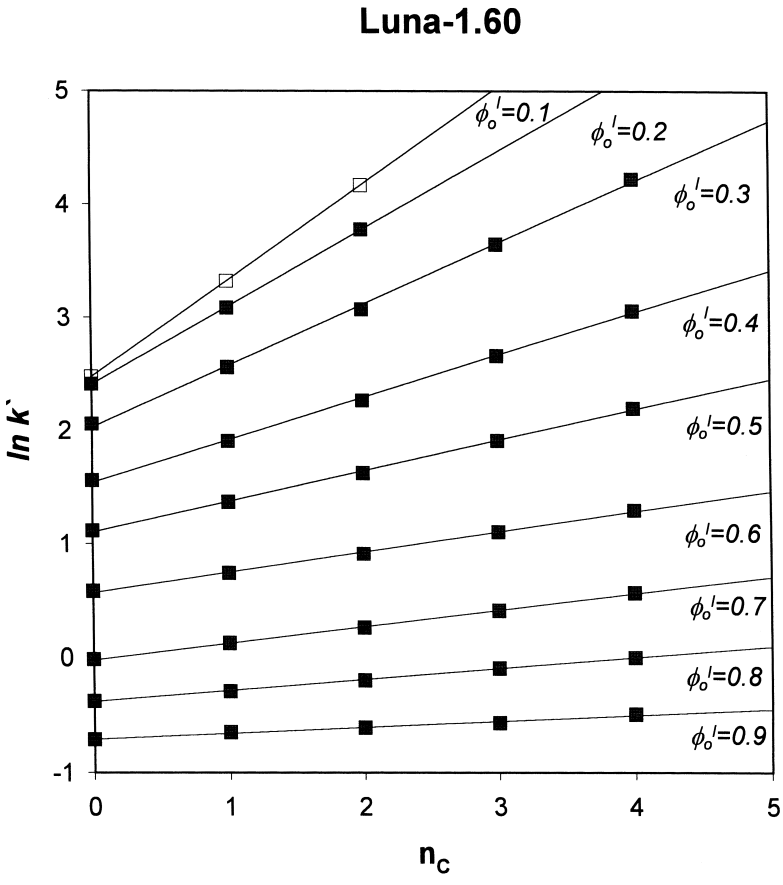

Fig. 8. Natural logarithm of the capacity factor for Luna-1.60 octyl phase as a function of the number of carbon atoms in the alkyl chain of homologous solutes.

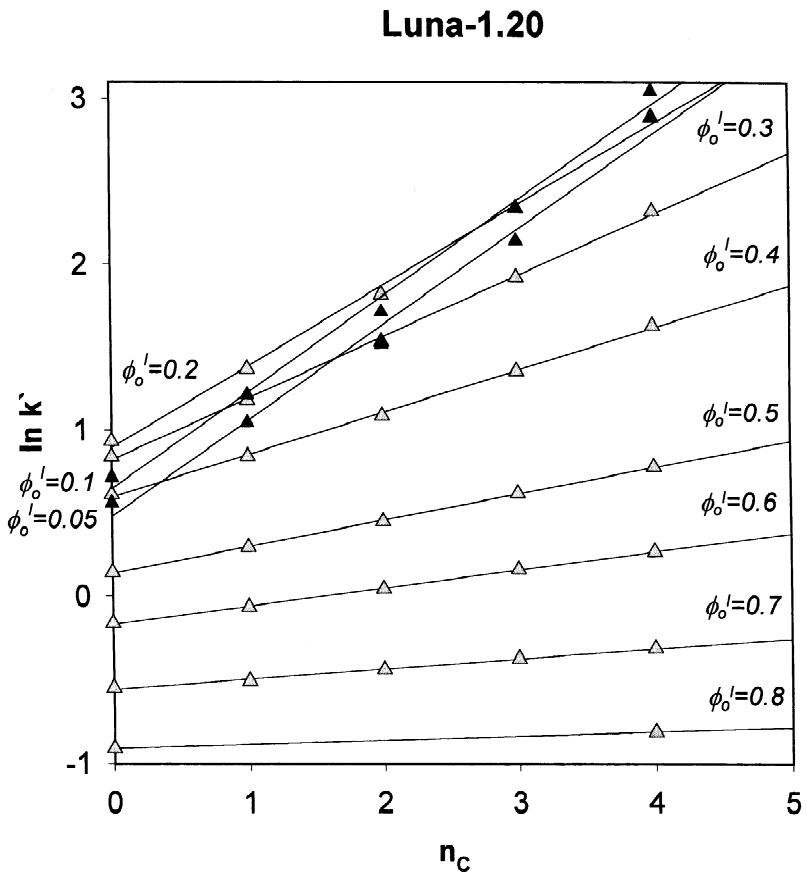

Fig. 9. Natural logarithm of the capacity factor for Luna-1.20 octyl phase as a function of the number of carbon atoms in the alkyl chain of homologous solutes.

taining 5% of acetonitrile, which showed that retention of benzene was even less than that for 10% solution. In Fig. 10 the capacity factors of benzene for all chromatographic systems are shown as a function of the mobile phase composition. A similar behavior was described in literature for methanol–water reversed-phase systems [29]. A decrease in the solute retention for predominantly aqueous mobile phase can be explained in terms of the immiscibility concept [16,24]. Thus, with increase of water concentration in the mobile phase the dispersive interactions of hydrophobic alkyl chains with themselves become significantly greater than interactions between alkyl chains and predominantly aqueous mobile phase. As a result of that the aliphatic chains collapse on the silica surface. Consequently, the effective surface area available for solute molecules is reduced, and the retention volume of a solute is decreased.

A collapsed state of hydrocarbon chains no longer allows to describe retention process in terms of the partition–displacement model, since at high water concentrations the retention mechanism could be regarded as essentially adsorption-like process. Therefore, in order to correctly use the partition–displacement model it was important to account for the change in the retention mechanism in the water rich mobile phase. Thus, in the partition–displacement model the slope of the ln k' dependence on the carbon number is typically used to estimate the logarithm of the methylene selectivity ($s = \ln \alpha_c = \mathrm{d} \ln k'/\mathrm{d}n_c$). For Luna-1.20 and Luna-1.60 phases the selectivity data for all mobile phase compositions, except acetonitrile concentrations of 20% and

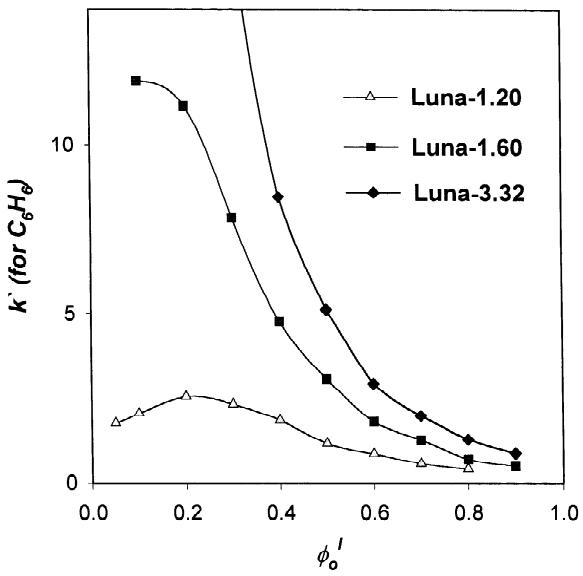

Fig. 10. The capacity factor of benzene as a function of mobile phase composition.

below, were used for this analysis. Fig. 11 shows the concentration range of the selectivity data, which were analyzed in terms of the partition–displacement model. For the octyl phases studied these data were used to determine the methylene selectivities in water and pure acetonitrile by extrapolating $\phi_o^{'}$ to zero and unity, respectively, (see Table 4). The extrapolated values were used to estimate the excess selectivity function (s_e) according to Eq. (2). It should be noticed that adsorption excess of acetonitrile is proportional to a negative quantity s_e. Hence, as can be concluded from Fig. 12 the stationary phase with the highest surface coverage of octyl phase (Luna-3.32) should exhibit the highest sorption excess of acetonitrile.

In addition to the qualitative evaluation of the sorption excess of acetonitrile from the excess selectivity data, the sorption constants of the octyl phases studied were estimated according to Eq. (5) (see Fig. 13). The sorption constants (Table 4) were

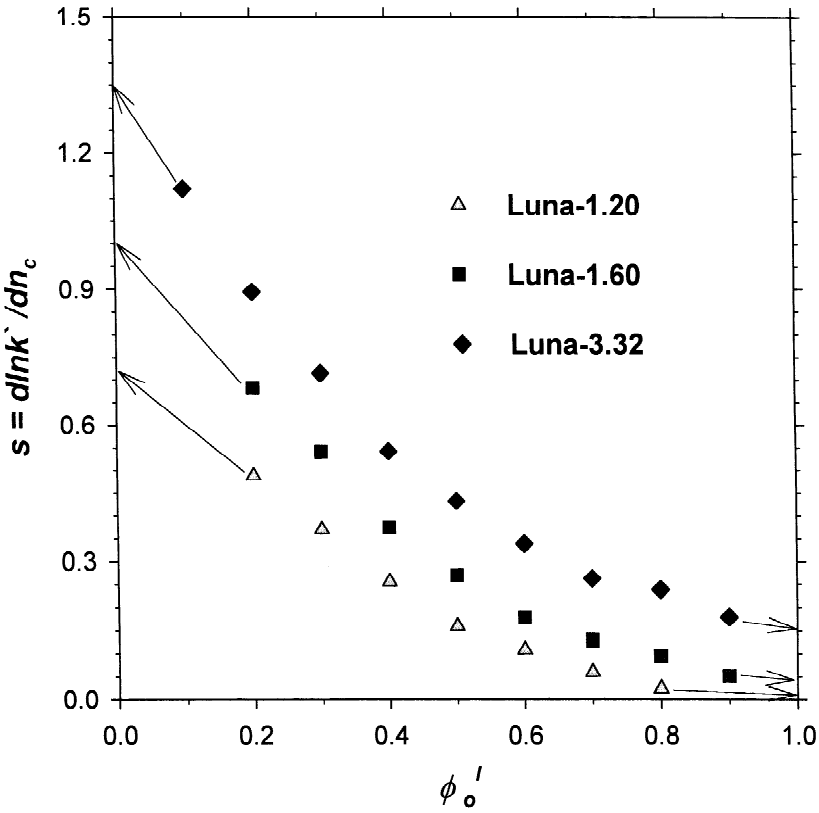

Fig. 11. Logarithm of the methylene selectivity as a function the mobile phase composition. Arrows show extrapolated values of the $s(\phi_o^{'})$ function.

Table 4
Chromatographic characterization of the octyl phases studied

Octyl phase	s_w	s_o	K_{ow}	r^2
Luna-1.20	0.72	0.01	1.44±0.12	0.990
Luna-1.60	1.00	0.04	1.63±0.09	0.989
Luna-3.32	1.35	0.16	1.80±0.12	0.995

used to calculate the fraction of acetonitrile in the stationary phase according to the Everett equation [7], and the sorption excess of acetonitrile in the stationary phase ($\phi_o^s - \phi_o^l$) as a function of the mobile phase composition. As can be seen in Fig. 14 for all systems the sorption excess of acetonitrile is positive, which indicates that acetonitrile is preferentially incorporated into the stationary phase. Moreover, the adsorption excess of acetonitrile shows a correlation with the surface coverage of the octyl phase, which is in agreement with the predic-

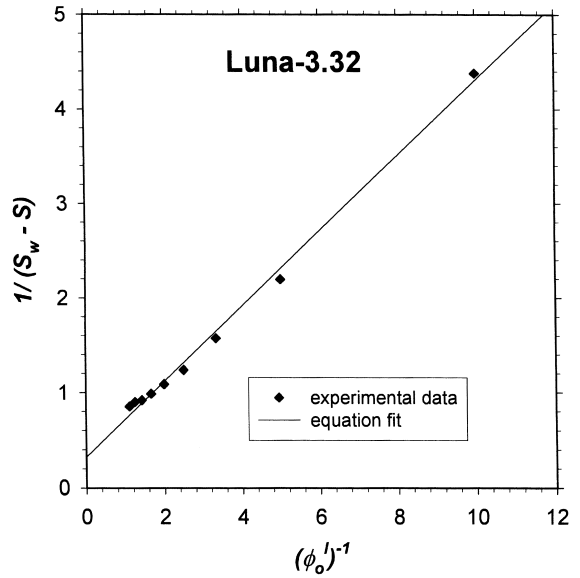

Fig. 13. Logarithmic methylene selectivity data fitted by Eq. (5).

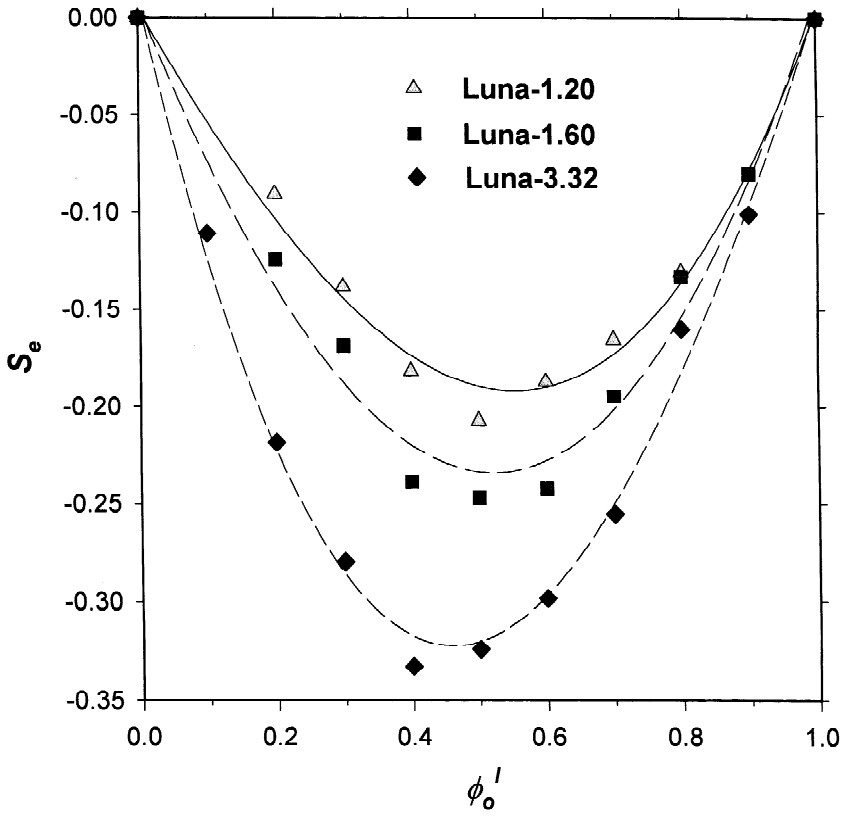

Fig. 12. Excess selectivity as a function the mobile phase composition.

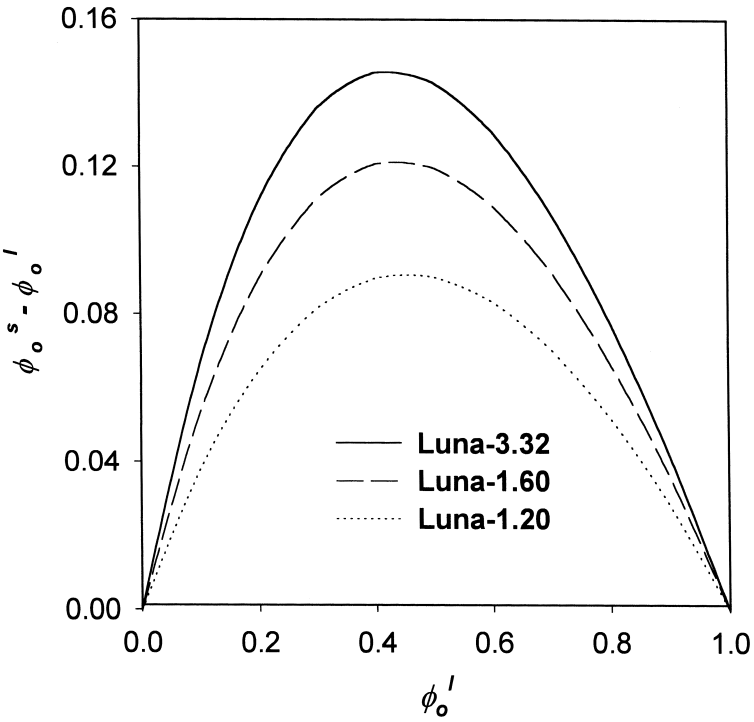

Fig. 14. Surface excess of acetonitrile as a function of the mobile phase composition.

tion based on the analysis of excess selectivity data. However, it should be mentioned that these conclusions are relevant for all measured mobile phase compositions in the case of high surface coverage octyl phase Luna-3.32, but in the case of low surface coverage phases Luna-1.60 and Luna-1.20 their applicability is restricted to acetonitrile rich compositions of the mobile phase.

4. Conclusions

Chemically bonded phases of different surface coverage were synthesized using the same support silica. Their surface and structural properties were characterized by means of nitrogen adsorption and solid-state NMR. Chromatographic properties of the synthesized silica-based octyl phases were evaluated using the partition–displacement model employed for analysis of methylene selectivity data obtained for a series of homologous alkyl benzenes.

Adsorption studies of the synthesized samples showed a decrease in the average pore diameter as a function of the increasing surface coverage, which proved that the modification of silica indeed proceeded inside of the porous structure of silica gel. Additionally, the low pressure adsorption isotherms were used to calculate the adsorption energy distributions for the derivatized silica samples. Analysis of the AEDs showed a decrease in the fraction of high adsorption energy sites with increase in the silica surface coverage. The changes in the AED spectra were correlated with a decreasing number of surface silanols as determined by CP-MAS-NMR experiments.

Further characterization of chromatographic packings consisted of evaluation of their methylene selectivity using retention measurements for homologous alkyl benzenes. The methylene selectivity data were used to estimate the sorption excess of acetonitrile in the stationary phase. Analysis of the excess curves showed that acetonitrile was preferentially adsorbed on the stationary phase, and the magnitude

of adsorption depends on the amount of surface hydroxyls and octyl phase coverage of the silica gel studied. Finally, chromatographic studies showed that application of the partition–displacement model for analysis of chromatographic packings of low surface coverage may be restricted to acetonitrile rich compositions of the mobile phase due to a change in the retention mechanism to an adsorption-like process when the concentration of acetonitrile in the mobile phase is low.

References

[1] L.R. Snyder, J.J.Kirkland, Introduction to Modern Liquid Chromatography, Wiley, New York, 1982.
[2] K. Robards, P.R. Haddad, P.E. Jackson, Principles and Practice of Modern Chromatographic Methods, Academic Press, San Diego, CA, 1994.
[3] U.D. Neue, HPLC Columns: Theory, Technology and Practice, Wiley, New York, 1997.
[4] P.W. Carr, D.E. Martire, L.R. Snyder (Guest Eds.), J. Chromatogr. A (1993) 656.
[5] J.G. Dorsey, W.T. Cooper, B.A. Siles, J.P. Folex, H.G. Barth, Anal. Chem. 68 (1996) 515R.
[6] L.C. Tan, P.W. Carr, M.H. Abraham, J. Chromatogr. A 752 (1996) 1.
[7] M. Jaroniec, J. Chromatogr. A 656 (1993) 37.
[8] M. Jaroniec, J. Chromatogr. A 722 (1996) 19.
[9] V. Bhagwat, Y. Bereznitski, B. Buszewski, M. Jaroniec, J. Liq. Chromatogr. 21 (1998) 923.
[10] T. Czajkowska, V. Tittelbach, Y. Bereznitski, M. Jaroniec, J. Liq. Chromatogr. 21 (1998) 1957.
[11] V. Bolis, A. Cavenago, B. Fubini, Langmuir 13 (1997) 895.
[12] I.S. Chuang, G.E. Macial, J. Phys. Chem. B 101 (1997) 3052.
[13] T. Takei, A. Yamazaki, T. Watanbe, M. Chikazawa, J. Colloid Interface Sci. 188 (1997) 409.
[14] A.Y. Fadeev, V. Eroshenko, J. Colloid Interface Sci. 187 (1997) 275.
[15] J. Nawrocki, J. Chromatogr. A 779 (1997) 29.
[16] R.P.W. Scott, Silica Gel and Bonded Phases, Wiley, Chichester, 1993.
[17] B. Buszewski, M. Jaroniec, R.K. Gilpin, J. Chromatogr. A 673 (1994) 11.
[18] D.H. Everett, J. Chem. Soc. Faraday. Trans. 60 (1964) 1803.
[19] S.J. Gregg, K.S.W. Sing, Adsorption Surface Area and Porosity, Academic Press, London, 1982.
[20] E.P. Barrett, L.G. Joyner, P.P. Halenda, J. Am. Chem. Soc. 73 (1951) 373.
[21] M.v. Szombathely, P. Brauer, M. Jaroniec, J. Comp. Chem. 13 (1992) 13.
[22] M. Jaroniec, R. Madey, Physical Adsorption on Heterogeneous Solids, Elsevier, Amsterdam, 1988.
[23] M. Mehring, NMR Spectroscopy in Solids, Springer–Verlag, New York, 1976.
[24] K. Albert, E. Bayer, J. Chromatogr. A 544 (1991) 345.
[25] A.B. Scholten, J.W. De Haan, H.A. Claessens, Langmuir 12 (1996) 4741.
[26] K.S.W. Sing, D.H. Everett, R.A.W. Haul, L. Moscou, R.A. Pierotti, J. Rouquerol, T. Sieminiewska, Pure Appl. Chem. 57 (1985) 603.
[27] Y. Bereznitski, M. Jaroniec, M. Kruk, J. Liq. Chromatogr. 19 (1996) 1523.
[28] Y. Bereznitski, M. Jaroniec, M. Kruk, B. Buszewski, J. Liq. Chromatogr. 19 (1996) 2767.
[29] C.H. Lochmuller, D.R. Wilder, J. Chromatogr. Sci. 17 (1979) 574.